

Strong guiding of light in hollow nanowire structures

Liang Chen¹, James De Leon², and Xiaomin Jin²

¹Nano Photonics, Inc., 21G Olympia Ave., Suite 50, Woburn, MA 01801, USA

²Electrical Engineering Department, California Polytechnic State University, San Luis Obispo, CA 93407, USA

Received July 10, 2007

We have theoretically investigated the guiding mode patterns of hollow nanowires. Two types of nanowires, round shape and hexagonal shape, are examined with different combination of outer and inner radii. Because of electric field discontinuity at hollow interfaces and evanescent modes overlap in low refractive index region, strong light guiding and confinement are achieved in both hollow wire structures.

OCIS codes: 230.0230, 220.0220, 230.1150.

Nanowires are one-dimensional (1D) nanostructures that can be synthesized by chemical vapor process^[1]. Through proper control of the growth process, doping, and other material parameters, one can create unique electronic and optical properties. These wires have several potential applications; the particular application of interest in photonics is in guiding the light. Nanowire waveguides synthesized as nanoribbon have been demonstrated in recent years^[2]. Conventionally, light will be confined in the high-index region of the waveguide because of total internal reflection. For solid nanowires, the optical modes will be expected to distribute along the nanowire like that in a dielectric waveguide. In contrast, a better optical field confinement and even a field enhancement are possible in the void (air) region of a hollow nanowire. It has been shown experimentally and theoretically that strong optical field can be confined in a low-index or void nanostructure^[3,4]. However their structures are based on slot rectangular waveguides. The similar effect is also expected in the hollow nanowires, which is surrounded by the high index contrast nanoshell. In practice, hollow nanowires can be created from the core/shell nanowire structure that has a low index core (air) at the center. GaN core/shell nanowires with a radial heterostructure have already been demonstrated^[5,6], which shows the feasibility of the hollow optical wire structure. To further understand the influence of the hollow structure on the light guiding properties of a nanowire, we have systematically studied the optical modes of circular and hexagonal hollow nanowire structures.

Our computation models for circular and hexagonal hollow nanowires are schematically shown in Fig. 1. It

consists of a nanowire with a refractive index of 2.55 (for example, index of GaN). The circular wire has an inner radius of r , and an outer radius of R . The hexagonal wire, on the other hand, has two characteristic dimensional parameters, D_a and d_a . In addition to the calculations on the circular and hexagonal shape nanowires, we have also performed calculations on circular solid wires for comparison. A full-vector finite-difference mode solver based on the two-dimensional (2D) Yee grid^[7] was implemented for calculating the transverse mode profiles and the corresponding dispersion relations for the circular and the hexagonal shape hollow as well as solid nanowires. Proper symmetry properties are explored to reduce the computation overhead.

In order to show whether the optical field can be confined or even enhanced in the low-index material with hollow-structure, we first simulated the electric field (E-field) intensity profile of circular and hexagonal hollow nanowires for variety of structures that have outer radius of 120 nm. The E-field intensities at the center of the hollow nanowire structures are much higher than that of the solid as seen in Figs. 2(a) and (b). At the mean time, the field is also confined in a much smaller region for the hollow structures as shown in Figs. 2(c) and (d) for circular and hexagonal structures. The enhancement of light confinement in the low index hollow region is due to the discontinuity of the E-field at the high index contrast interfaces as proposed in Refs. [3, 4]. The maximum ratio of peak E-field component normal to the discontinuities is n_H^2/n_L^2 ^[3]. However, our calculation further shows that the center E-field in the hollow structure is made up by the evanescent mode overlapping. The closer the discontinuities, the higher the enhancement. As shown in Fig. 2(c), the E-field reaches its maximum value at the discontinuous point and decays. Because of all evanescent modes overlapping at the center, when the size of hollow structure shrinks, the E-field enhances. Since the evanescent modes exist in a very small nano-range, this E-field intensity enhancement exists only in the nano-hollow structure. This is further verified by studying the influence of inner aperture size on the enhancement of center E-field. We have calculated a variety of circular nanowire structures with outer radii of 60, 90, and 120 nm and inner radii sweeping from 5 to 40 nm. Figure 3 shows the hollow-

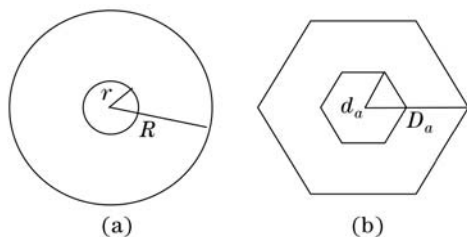


Fig. 1. (a) Schematic of a circular cross-section hollow nanowire used in the calculation. (b) Schematic of a hexagonal cross-section hollow nanowire used in the calculation, where D_a and d_a are two characteristic lateral sizes defined in the calculation.

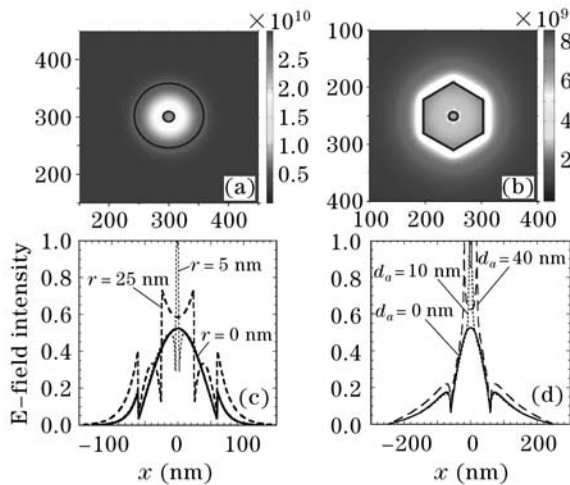


Fig. 2. E-field intensity profiles of HE_{11} mode of (a) hollow circular and (b) hollow hexagonal nanowire structures. (c) The E-field intensity distribution of HE_{11} mode of circular hollow nanowires with $R = 60$ nm for $r = 0, 5$, and 25 nm at 400 -nm wavelength. (d) The E-field intensity distribution of HE_{11} mode of hexagonal hollow nanowires with $D_a = 120$ nm for $d_a = 0, 10$, and 40 nm at 400 -nm wavelength.

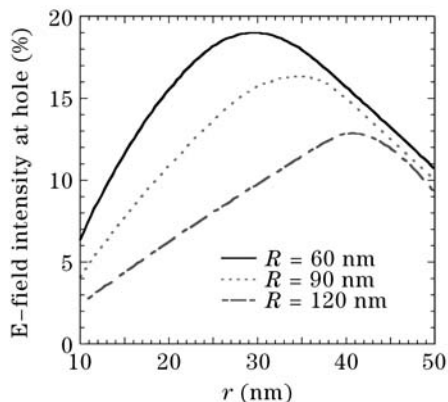


Fig. 3. Percentage of E-field intensity of HE_{11} mode at hollow nanowires region normalized to the total E-field of the whole structure for $R = 60, 90$, and 120 nm with different inner radii at 400 -nm wavelength.

region E-field intensity as function of structure size (R) and aperture size (r). As the structure size increases, the effect of E-field enhancement becomes less pronounced. This is due to the evanescent modes in the hollow range is small or E-field is more confined in the ring for large structure. When the aperture is too small, even the E-field intensity is the highest; the percentage of the E-field at the hole according to the total E-field integration is still small. When the aperture size is too large, the E-field decreases as well. This is due to the large separation between two index discontinuities, where E-field decays exponentially toward outside of the high index materials. Overall, a maximum E-field percentage can be achieved when varying aperture size.

To understand the mode operation range of the hollow structure, we calculate the effective indices of HE_{11} , TE_{01} , and TM_{01} modes for different aperture sizes, as shown in Fig. 4(a). To realize the single mode operation, the normalized frequency should be smaller than 0.1667 , which is above 417 nm in wavelength. It can also be

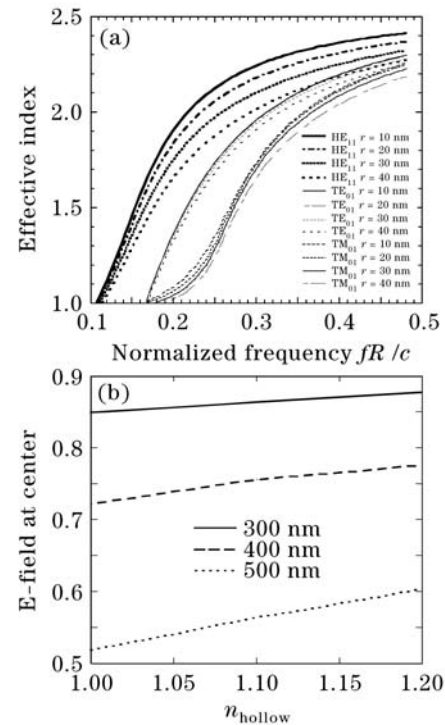


Fig. 4. (a) Effective index of refraction of circle hollow nanowire structures with $R = 120$ nm, and $r = 10, 20, 30$, and 40 nm. (b) HE_{11} mode E-field variation of $D_a = 120$ nm hexagonal hollow nanowire structure when hollow area index changes at wavelengths of $300, 400$, and 500 nm.

seen that the effective index of HE_{11} mode has much stronger dependence on the size of the center hole. This is because that the E-field of HE_{11} mode is linearly polarized across the hollow hole, which results in the discontinuity of field intensity and hence the confinement as well as enhancement at the hollow center. Contrarily the E-field of TE_{01} mode is circularly surrounding the center hole and no normal component is available to cross the semiconductor-hollow interface. This results in that the mode profile of TE_{01} mode is insensitive to the existence of the center hole, so is the effective index. For TM_{01} mode, since the major component of the E-field is along the axial direction, which is parallel to the semiconductor-hollow interfaces, the effect of the hollow region is also minimal. The strong dependence of the HE_{11} optical mode on the existence of the center hollow region makes it very useful in optical sensor applications. For example, if we use the nanowire structure as a sensor, we can monitor the center optical field strength as a function of the refractive index of the center hole to measure the variation happened there. Figure 4(b) is the optical field intensity of HE_{11} mode versus the material index of the center hollow region at different wavelengths. The center optical field intensity shows strong dependence on the refractive index of the hollow material at all three wavelengths. This verifies the feasibility of using hollow nanowires in the sensor applications.

In summary, our simulation shows that there are strong light guiding and optical confinement in the low refractive index region, which is similar to the slot waveguide structures. The enhancement of light confinement in the low index nanoscale hollow region is due to the E-field

discontinuity at the high index contrast interfaces and possible evanescent-mode summation for the nano-hollow structure. The E-field intensities at the center of the hollow nanowire structures are much higher than that of the solid nanowire. At the mean time, the field is also confined in a much smaller region for the hollow structures. The strong confinement of optical field in the center of hollow nanowires makes them very promising candidates in the application of nano-sensors.

We thank Wang Faculty Fellowship 2006 – 2007 through California State University International Programs (USA) and Agilent Global Research Funding for the support of this research. X. Jin is the author to whom the correspondence should be addressed, her e-mail address is xjin@calpoly.edu.

References

1. M. Law, J. Goldberger, and P. D. Yang, *Annu. Rev. Mater. Res.* **34**, 83 (2004).
2. M. Law, D. J. Sirbulu, J. C. Johnson, J. Goldberger, R. J. Saykally, and P. D. Yang, *Science* **305**, 1269 (2004).
3. Q. Xu, V. R. Almeida, R. R. Panepucci, and M. Lipson, *Opt. Lett.* **29**, 1626 (2004).
4. V. R. Almeida, Q. Xu, C. A. Barrios, and M. Lipson, *Opt. Lett.* **29**, 1209 (2004).
5. F. Qian, S. Gradecak, Y. Li, C. Y. Wen, and C. M. Lieber, *Nano Lett.* **5**, 2287 (2005).
6. F. Qian, Y. Li, S. Gradecak, D. Wang, C. J. Barrelet, and C. M. Lieber, *Nano Lett.* **4**, 1975 (2004).
7. Z. M. Zhu and T. G. Brown, *Opt. Express* **10**, 853 (2002).